

**Figure 8.** Homonuclear 2D proton MAS results in hydrated H-rho. Shown are two cross sections through the diagonal peaks of the 2D spectrum obtained from 64 FID's with 24 scans each:  $\tau = 0.5$  ms; delay 0.5 s;  $t_1$  increments 60  $\mu$ s; dwell time 30  $\mu$ s.

between hydrated H-rho and anhydrous  $\text{NH}_4$ -rho, where the  $^{29}\text{Si}$  spectrum of the latter is also less resolved and shifted to lower field by 4 ppm.<sup>14</sup> This framework deformation is related to the exceptional flexibility of the rho lattice where the double eight-rings can be circular or elliptical.<sup>13,30</sup> Ellipticity is induced in anhydrous  $\text{NH}_4$ -rho by the ammonium ions that are located at the centers of the eight-rings.<sup>30</sup> We may, therefore, speculate that the "nonuniform" framework components in hydrated H-rho are substructures with strongly coordinating ligands in the eight-rings. These then carry the 9-ppm hydroxyl groups. Further speculation about their nature is obviously not warranted, although we may recall at this point that  $^{27}\text{Al}$  NMR has shown the samples to contain nearly two aluminum atoms per unit cell in a highly symmetric octahedral coordination.<sup>14</sup> Two-dimensional  $^1\text{H}$ - $^{27}\text{Al}$  spectroscopy can perhaps contribute to a better understanding of

this aspect of the zeolite structure.

### Conclusions

The examples presented in this paper demonstrate that the interpretation of proton MAS spectra of surface species on siliceous substrates can be aided by  $^1\text{H}$ - $^{29}\text{Si}$  double-resonance experiments. The methodology includes CP/MAS  $^{29}\text{Si}$  experiments with varying contact time and corresponding heteronuclear 2D spectroscopy. While the former may reveal  $^{29}\text{Si}$  subspectra of sample components with different degrees of association with proton-containing groups, the later selectively identifies the chemical shifts of the protons that are rigidly bound to these substrate components.

The method was proved to be useful for the structural characterization of hydrated zeolites, where it was shown that the bulk water in the cavities is not a source for  $^{29}\text{Si}$  cross polarization. This was found for the hydrated zeolites Na-A, Ca,Na-A,  $\text{NH}_4$ -rho, and with some uncertainty for H-rho. When cross polarization did occur, we could identify the MAS peak of the corresponding structural hydroxyl. In Ca,Na-A this hydroxyl group is evidently associated with the main zeolite framework, because the CP  $^{29}\text{Si}$  spectrum is identical with the single-pulse-excitation spectrum. In hydrated H-rho the results revealed a newly observed nonuniform framework component, and the OH signal of each component was identified.

Since proton spin exchange during the CP contact time obscures the selectivity of the 2D experiment, a homonuclear 2D proton experiment could be valuable for the independent confirmation of exchange. An example is hydrated H-rho where water appears to contribute to cross polarization. The proton 2D data are, however, inconclusive in this case, because of the proximity and the intensity difference of the two peaks involved.

**Acknowledgment.** I thank D. R. Corbin and R. D. Shannon for providing samples and also P. J. Domaille, R. D. Farlee, D. C. Roe, and D. L. VanderHart for helpful discussions. The highly skilled technical assistance of R. O. Balback is greatly appreciated.

**Registry No.** Silica, 7631-86-9.

(30) McCusker, L. B. *Zeolites* 1984, 4, 51.

## The $^{31}\text{P}$ Chemical Shielding Tensor in Phospholipids<sup>||</sup>

H. Hauser,<sup>†</sup> C. Radloff,<sup>†</sup> R. R. Ernst,<sup>\*†</sup> S. Sundell,<sup>§</sup> and I. Pascher<sup>§</sup>

*Contribution from the Laboratorium für Biochemie und Laboratorium für Physikalische Chemie, Eidgenössische Technische Hochschule, 8092 Zürich, Switzerland, and the Department of Structural Chemistry, Faculty of Medicine, University of Göteborg, Box 33031 S-40033 Göteborg, Sweden. Received April 1, 1987*

**Abstract:** The  $^{31}\text{P}$  chemical shielding tensor has been determined for single crystals of 1-hexadecyl-2-deoxyglycerophosphoric acid monohydrate, an analogue of the naturally occurring phosphatidic acid. The measured values for the principal components of the shielding tensor are -53, -2, and +58 ppm relative to 85%  $\text{H}_3\text{PO}_4$ . It is found that its principal axes coincide within  $2^\circ$  with a Cartesian coordinate system defining the symmetry of the phosphate group. The orientation of the chemical shielding tensor of 1-hexadecyl-2-deoxyglycerophosphoric acid is similar to that measured in single crystals of other phosphomonoesters, such as phosphoethanolamine, phosphoserine, 3'-cytidine monophosphate, and deoxy 5'-monophosphate. These compounds are water-soluble polar molecules and have no hydrocarbon chains, contrary to 1-hexadecyl-2-deoxyglycerophosphoric acid. The orientation of the chemical shielding tensor of 1-hexadecyl-2-deoxyglycerophosphoric acid differs only by  $7$ - $13^\circ$  from that of the phosphodiester barium diethyl phosphate, which has been used as a model for the  $^{31}\text{P}$  chemical shielding tensor of phospholipids.

### 1. Introduction

Phosphorus-31 NMR has been widely used in the structure elucidation of phospholipid bilayers and biological membranes. In particular, the anisotropy of the  $^{31}\text{P}$  chemical shielding tensor

allows one to deduce information on conformation and orientation of the phospholipid molecules in these anisotropic structures. In order to exploit this source of information, it is necessary to know the orientation of the shielding tensor within the molecular framework. Because computational approaches are unfeasible, it is necessary to determine the orientation of the shielding tensor experimentally on suitable model systems.

A principal problem in the experimental determination of the tensor orientation is the extreme difficulty to grow single crystals sufficiently large for NMR investigations. So far, single crystals

<sup>||</sup> This paper is dedicated to Professor Giorgio Semenza on the occasion of his 60th birthday.

<sup>†</sup> Laboratorium für Biochemie, Eidgenössische Technische Hochschule.

<sup>†</sup> Laboratorium für Physikalische Chemie, Eidgenössische Technische Hochschule.

<sup>§</sup> Department of Structural Chemistry, University of Göteborg.

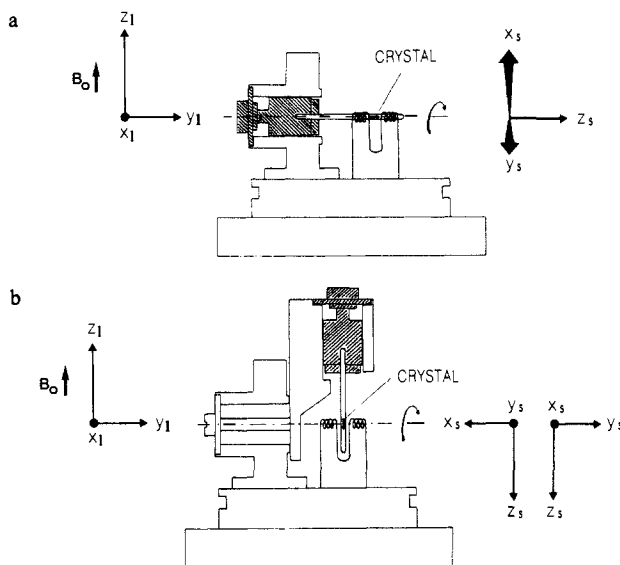


**Figure 1.** Schematic drawing of the <sup>31</sup>P NMR probe goniometer. (a) The HPA2 single crystal is enclosed in a 2-mm glass capillary which is cemented into a sample holder of quadratic cross section made of Kel-F (shaded part). The sample holder has been designed such that it is transferable between NMR probe and X-ray goniometer. The sample holder is inserted into the NMR goniometer in such a way that the long axis of the glass capillary is parallel to the rotation axis of the NMR goniometer (--- in the figure). Also shown (right-hand side) is the sample frame, which is defined with the z axis z<sub>s</sub> being parallel to the goniometer rotation axis. On the left-hand side are shown the direction of the magnetic field B<sub>0</sub> and related to it the laboratory frame. (b) The orientation of the glass capillary is perpendicular to the rotation axis of the NMR goniometer. Two such perpendicular orientations are possible as indicated by the two different sample frames shown on the right. The perpendicular orientations are achieved by inserting the sample holder (shaded part) in an auxiliary attachment. For this a special design of the radio-frequency coil was necessary.

of phospholipids have been small and of poor quality by normal crystallographic standards.<sup>1</sup> For this reason, Griffin et al.<sup>2,3</sup> have determined the <sup>31</sup>P shielding tensor on the somewhat oversimplified model system of barium diethyl phosphate, of which large crystals can be grown. It is likely that this is a fair model for phosphodiester of lipids as the principal values of the shielding tensor are close to those derived from powder spectra of phospholipids.

In order to allow the comparison with a phospholipid, we set out to grow single crystals of 1-hexadecyl-2-deoxyglycerophosphoric acid monohydrate (HPA), an analogue of the naturally occurring phosphatidic acid. Both are phosphomonoesters. The results of a determination of the <sup>31</sup>P chemical shielding tensor are reported in this paper. The success hinged on the construction of a new goniometer probe assembly designed for rotation about three axes of tiny crystals embedded in a capillary tube.

## 2. Experimental Section

**2.1. Design of Goniometer Probe for NMR Measurements.** The design criteria for the goniometer probe assembly were (i) the possibility to rotate a small crystal fixed in a 2-mm capillary tube about orthogonal axes and (ii) easy transfer of the sample between X-ray goniometer and NMR probe. Figure 1 illustrates the basic idea. The capillary tube is fixed to a sample holder of quadratic cross section made of Kel-F (shaded part in Figure 1). The sample holder is transferable between X-ray goniometer and NMR probe. It can be inserted in three orthogonal positions into the NMR goniometer. The orientation of the capillary perpendicular to the rotation axis (Figure 1b) is achieved with an auxiliary attachment and with a specially designed split radio-frequency coil that allows insertion of the capillary in parallel and perpendicular orientation. The NMR goniometer is oriented with its rotation axis per-

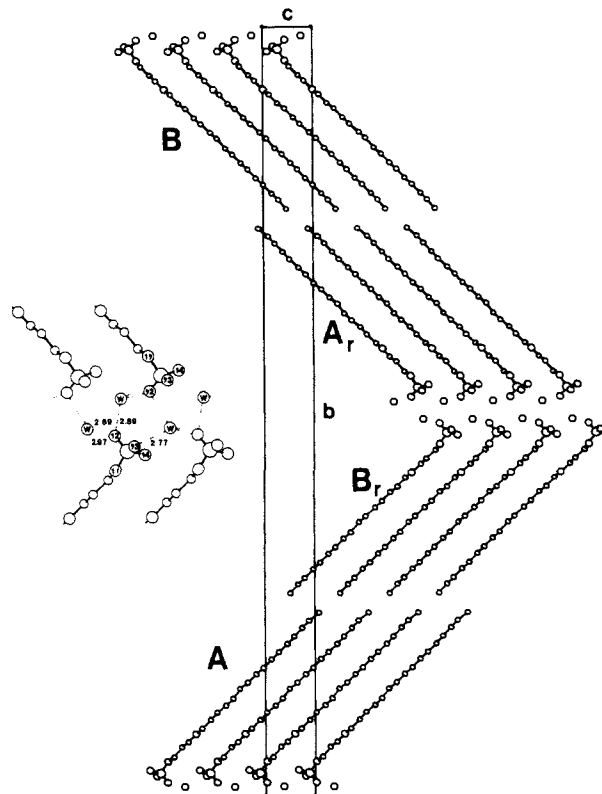


**Figure 2.** Molecular packing in HPA2 viewed along a direction perpendicular to the bc plane. HPA2 crystals are monoclinic, belonging to space group P2<sub>1</sub>. The box is the bc plane of the unit cell with axes a = 4.76 Å, b = 88.83 Å, and c = 5.72 Å; β = 100.48°. Inset: expanded version of the interfacial region of two neighboring bilayers. The numbering of the O atoms is according to Pascher et al.<sup>4</sup> Hydrogen bonds are indicated by dotted lines, and some of their distances are given in angstroms. Hydrogen bonds extending in the a direction are indicated by interrupted lines. W = water molecule of hydration.

pendicular to the magnetic field B<sub>0</sub>.

Although compromises had to be made in the design of the radio-frequency coil, the sensitivity is surprisingly good. This can be appreciated from the fact that a spectrum as the one shown in Figure 3 was obtainable in 30 min using a crystal with a volume of 0.24 mm<sup>3</sup>.

**2.2. Single Crystals of 1-Hexadecyl-2-deoxyglycerophosphoric Acid Monohydrate.** The synthesis of 1-hexadecyl-2-deoxyglycerophosphoric acid (HPA) was described previously.<sup>4</sup> Single crystals of HPA were grown from dichloromethane-ethane-H<sub>2</sub>O (10:1.5:0.1 by volume) solutions; 10 mg of HPA was dissolved in 1.5 mL of solvent at 50 °C, and crystallization was induced by cooling the lipid solution to 20 °C within about 12 h.

Two crystal forms are obtained, depending on the temperature of growth. Below 8 °C the compound crystallizes in a triclinic form (HPA1) while at 20 °C a monoclinic crystal (HPA2) is obtained in the form of thin plates. The structure of both forms has been determined previously.<sup>4</sup> While all molecules are magnetically equivalent in the triclinic form, the monoclinic form contains two magnetically inequivalent molecules.

Unfortunately, it proved impossible to obtain sufficiently large crystals of the simpler form HPA1, and it was necessary to make the measurements on the monoclinic form HPA2. This introduces an inherent assignment problem to be discussed later.

The HPA2 crystal used for the NMR measurements was of dimensions 4.2 × 2.4 × 0.024 mm. The unit cell dimensions of this crystal were determined as a = 4.76 Å, b = 88.83 Å, and c = 5.72 Å, with β = 100.48°, in agreement with published data.<sup>4</sup>

The packing of the HPA molecules in the unit cell is shown as a projection onto the bc plane in Figure 2. The unit cell contains four molecules which are packed pairwise in two adjacent bilayers. These two bilayers differ in the tilt of the hydrocarbon chains, giving rise to a herringbone-like arrangement. The long unit cell axis b apparently spans two bilayers. The molecules A and B are crystallographically related to

(1) Hauser, H.; Pascher, I.; Pearson, R. H.; Sundell, S. *Biochim. Biophys. Acta* **1981**, *650*, 21-51.

(2) Herzfeld, J.; Griffin, R. G.; Haberkorn, R. A. *Biochemistry* **1978**, *17*, 2711-2718.

(3) Griffin, R. G. In *Methods Enzymol.* **1981**, *72*, 108-174.

(4) Pascher, I.; Sundell, S.; Eibl, H.; Harlos, K. *Chem. Phys. Lipids* **1984**, *35*, 103-115.

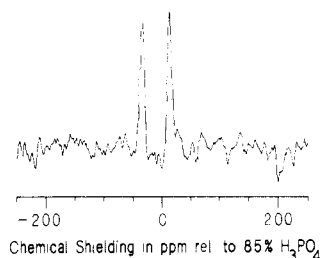


**Figure 3.**  $^{31}\text{P}$  NMR spectrum recorded from a HPA2 single crystal at room temperature. The two lines of width at half-height of about 4 ppm arise from the magnetically inequivalent HPA molecules in the unit cell. The spectrum was obtained with the goniometer rotation axis parallel to  $z_1$  (cf. Figure 1). The chemical shielding is expressed in ppm with respect to external 85%  $\text{H}_3\text{PO}_4$ .

**Table I.** Rotation Matrix  $\mathbf{R}^{(cp)}$  Relating the Principal Axes Frame ( $x_p, y_p, z_p$ ) to the Crystal Frame ( $a, b, c'$ )

| molecule | U  | V  |                             |                             |
|----------|----|--|-----------------------------|-----------------------------|
|          |    | $x_p$ ( $\sigma_{11}$ axis) <sup>a</sup> | $y_p$ ( $\sigma_{22}$ axis) | $z_p$ ( $\sigma_{33}$ axis) |
| A        | a  | $0.708 \pm 0.007$                        | $0.480 \pm 0.003$           | $-0.518 \pm 0.012$          |
|          | b  | $-0.026 \pm 0.016$                       | $0.753 \pm 0.003$           | $0.658 \pm 0.032$           |
|          | c' | $0.705 \pm 0.007$                        | $-0.453 \pm 0.008$          | $0.546 \pm 0.027$           |
| B        | a  | $0.713 \pm 0.012$                        | $0.460 \pm 0.008$           | $0.530 \pm 0.008$           |
|          | b  | $0.327 \pm 0.051$                        | $-0.885 \pm 0.005$          | $0.332 \pm 0.012$           |
|          | c' | $0.622 \pm 0.016$                        | $-0.064 \pm 0.008$          | $-0.781 \pm 0.001$          |

<sup>a</sup>The matrix elements are identical with the direction cosines; e.g.,  $\cos(\mathbf{ax}_p) = 0.708$ .

the molecules A, and B, respectively, in the adjacent bilayer by a twofold screw axis which coincides with the  $b$  axis. The molecules A and B, themselves are related by a noncrystallographic center of symmetry and are magnetically equivalent as well as the molecules A, and B. As a consequence, there are two magnetically inequivalent phosphate groups in the sample. The insert in Figure 2 shows an expansion of two neighboring layers of phosphate groups together with the water molecules of hydration and the hydrogen-bonding network (dotted lines).

**2.3. Measurement of the Chemical Shielding Tensor.** The single crystal of HPA2 was inserted in arbitrary orientation into a glass capillary and glued to the glass wall. One end of the capillary was sealed, and the other end was cemented into the Kel-F sample holder. The orientation of the unit cell axes  $a, b, c$  with respect to the sample holder frame  $x_s, y_s, z_s$ , indicated in Figure 1, was determined by X-ray diffraction before and after the NMR measurements. This ensured that the crystal orientation remained unchanged in its position within the glass capillary during the measurement.

The  $^{31}\text{P}$  NMR measurements were made on a Bruker CXP 300 spectrometer operating at a  $^{31}\text{P}$  frequency of 121.47 MHz. The phosphorus signal was enhanced by Hartmann-Hahn cross polarization between protons and phosphorus, and proton spin decoupling was employed during data acquisition. Spectra were recorded for 20 crystal orientations for each of the three orthogonal rotations. For the two mountings of the single-crystal shown in parts a and b of Figure 1, 500 and 1500 free induction decays, respectively, were coadded for each orientation, with a waiting time of 3 s between measurements.

A typical single-crystal spectrum is given in Figure 3. Two lines originating from the two magnetically inequivalent sites are visible. Figure 4 shows the three rotation plots for both sites. For a cross check, a powder spectrum, represented in Figure 5, was recorded.

### 3. Determination of the Chemical Shielding Tensor

At first, a rough estimate of the principal axis values of the shielding tensor was determined by fitting the powder spectrum of Figure 5 by computer simulations. The fit shown in Figure 5, obtained with a Gaussian broadening function, is not perfect. It is likely that it could be improved by modifying the line-shape function. Because the obtained principal axis values, contained in Table I, served merely as cross checks, no further effort was invested to improve the fit.

For the computation of the principal axis values and of the orientation angles of the chemical shielding tensor,  $\sigma$ , from the three rotation plots, the coordinate systems indicated in Figure 6 are relevant. The sample frame ( $x_s, y_s, z_s$ ), also indicated in Figure 1, is related to the laboratory frame ( $x_l, y_l, z_l$ ) by the transformation  $\mathbf{R}^{(ls)}$ , expressing a rotation of angle  $\phi$  about the

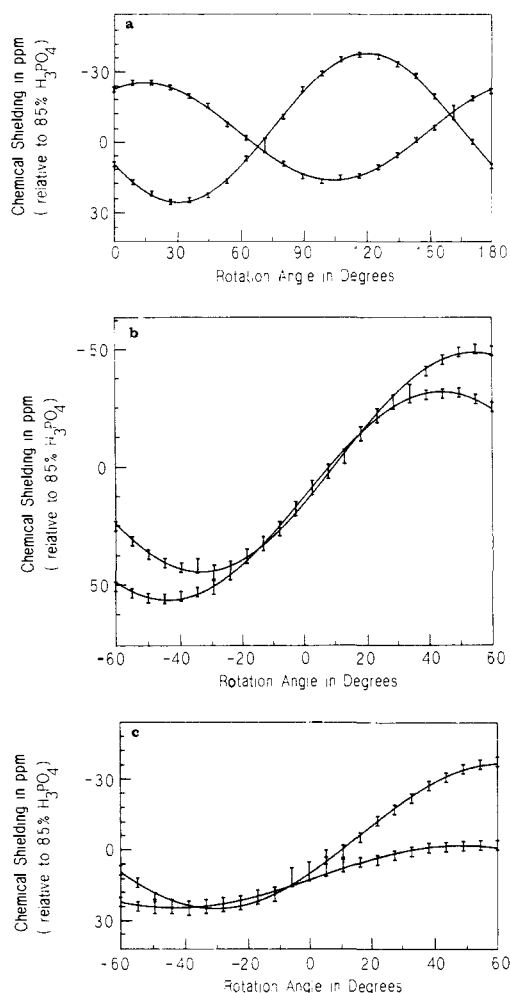


**Figure 4.** Rotation plots relating the observed  $^{31}\text{P}$  chemical shielding to the angle of rotation  $\phi$ . The HPA2 single crystal was rotated about the rotation axis of the NMR goniometer as shown in Figure 1. Chemical shielding was measured relative to external 85%  $\text{H}_3\text{PO}_4$ . In (a) the rotation axis of the goniometer is parallel to the  $z$  axis of the sample frame ( $z_p$ ), and in (b) and (c) it is parallel to  $x_p$  and  $y_p$ , respectively. The experimental points and error bars are given together with the theoretical curves computed by a least-squares analysis using eq 5-7.

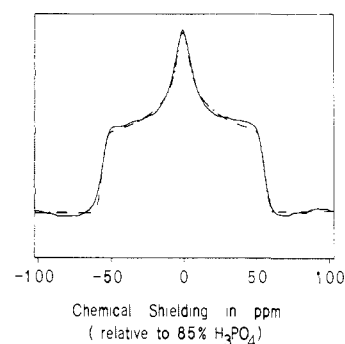


**Figure 5.** Axially asymmetric  $^{31}\text{P}$  powder NMR spectrum obtained with a powder of monoclinic HPA2 at room temperature (solid line). Chemical shielding is expressed in ppm relative to external 85%  $\text{H}_3\text{PO}_4$ . Also included is a computer simulation of the powder spectrum (---) using a Gaussian broadening function. The values of the principal components of the  $^{31}\text{P}$  chemical shielding tensor in HPA2 derived from this computer simulation are included in Table I.

goniometer axis, and by a cyclic permutation of the three axis that depends on the position of the sample holder in the goniometer:

$$\mathbf{R}^{(ls)} = \mathbf{R}(\phi)\mathbf{P}(x,y,z) \quad (1)$$

with

$$\mathbf{R}(\phi) = \begin{bmatrix} \cos \phi & 0 & -\sin \phi \\ 0 & 1 & 0 \\ \sin \phi & 0 & \cos \phi \end{bmatrix} \quad (2)$$

and, e.g.

$$\mathbf{R}^{(ls)} = \begin{bmatrix} -\sin \phi & \cos \phi & 0 \\ 0 & 0 & 1 \\ \cos \phi & \sin \phi & 0 \end{bmatrix} \quad (3)$$

for the rotation about the z<sub>s</sub> axis. The indices l,s on the rotation matrices **R**<sup>(ls)</sup> indicate destination and origin of the transformation; for example

$$\sigma^{(l)} = \mathbf{R}^{(ls)} \sigma^{(s)} \mathbf{R}^{(ls)-1} \quad (4)$$

The transformation matrix **R**<sup>(sc)</sup>, which transforms the crystal frame<sup>12</sup> (a, b, c') into the sample frame (x<sub>s</sub>, y<sub>s</sub>, z<sub>s</sub>), has been determined by X-ray diffraction.

The desired quantities are the eigenvalues of the tensor σ, as well as the orientation of the principal axes frame with respect to the crystal frame, expressed by the transformation matrix **R**<sup>(cp)</sup>. In the present approach, we determined first the tensor σ<sup>(s)</sup> by a least-squares fit of the shielding values measured for the different orientations of the crystal. By a subsequent diagonalization σ<sup>(p)</sup> and **R**<sup>(sp)</sup> are found. From **R**<sup>(sp)</sup> and the known **R**<sup>(sc)</sup> finally **R**<sup>(cp)</sup> is computed.

The experimentally accessible shielding value is given by the matrix element σ<sub>33</sub><sup>(l)</sup>. It can be expressed by means of eq 1-4 in terms of the matrix elements of σ<sup>(s)</sup>:

$$\sigma_{33}^{(l)}(x_s) = \frac{1}{2}(\sigma_{22}^{(s)} + \sigma_{33}^{(s)}) + \frac{1}{2}(\sigma_{33}^{(s)} - \sigma_{22}^{(s)}) \cos 2\phi + \frac{1}{2}(\sigma_{23}^{(s)} + \sigma_{32}^{(s)}) \sin 2\phi \quad (5)$$

$$\sigma_{33}^{(l)}(y_s) = \frac{1}{2}(\sigma_{33}^{(s)} + \sigma_{11}^{(s)}) + \frac{1}{2}(\sigma_{33}^{(s)} - \sigma_{11}^{(s)}) \cos 2\phi + \frac{1}{2}(\sigma_{13}^{(s)} + \sigma_{31}^{(s)}) \sin 2\phi \quad (6)$$

$$\sigma_{33}^{(l)}(z_s) = \frac{1}{2}(\sigma_{11}^{(s)} + \sigma_{22}^{(s)}) + \frac{1}{2}(\sigma_{11}^{(s)} - \sigma_{22}^{(s)}) \cos 2\phi + \frac{1}{2}(\sigma_{12}^{(s)} + \sigma_{21}^{(s)}) \sin 2\phi \quad (7)$$

The axis about which the crystal is rotated is indicated in parentheses. Symmetry of the shielding tensor is enforced by setting σ<sub>23</sub><sup>(s)</sup> = σ<sub>32</sub><sup>(s)</sup>, σ<sub>13</sub><sup>(s)</sup> = σ<sub>31</sub><sup>(s)</sup>, and σ<sub>12</sub><sup>(s)</sup> = σ<sub>21</sub><sup>(s)</sup>. It is then possible to fit the shieldings for the n measured orientations by expressing σ<sub>33k</sub><sup>(l)</sup> in terms of the six unknown parameters **p** = (σ<sub>11</sub><sup>(s)</sup>, σ<sub>22</sub><sup>(s)</sup>, σ<sub>33</sub><sup>(s)</sup>, σ<sub>12</sub><sup>(s)</sup>, σ<sub>13</sub><sup>(s)</sup>, σ<sub>23</sub><sup>(s)</sup>):

$$\sigma_{33}^{(l)} = \mathbf{A} \mathbf{p} \quad (8)$$

where **A** is a n × 6 matrix formed by coefficients contained in eq5-7. A standard least-squares fitting procedure leads to the parameter vector **p** in the form

$$\mathbf{p} = (\mathbf{A}^T \mathbf{A})^{-1} \mathbf{A}^T \sigma_{33}^{(l)} \quad (9)$$

This determines the tensor σ<sup>s</sup>, which is subsequently diagonalized:

$$\sigma^{(p)} = \mathbf{R}^{(sp)-1} \sigma^{(s)} \mathbf{R}^{(sp)} \quad (10)$$

Finally, the orientation of the shielding tensor in the crystal axes frame, expressed by the rotation matrix **R**<sup>(cp)</sup>, is obtained in the form

$$\mathbf{R}^{(cp)} = \mathbf{R}^{(sc)-1} \mathbf{R}^{(sp)} \quad (11)$$

The results of this fitting procedure are given in Table I. The errors of the determined parameters are expressed by their standard deviation calculated by the error propagation laws.

Two independent calculations have been done for the two not yet assigned crystal sites. The assignment given in Table I and Figure 7 was reached as follows: It can be expected that the chemical shielding tensor should conform to the local symmetry of the PO<sub>4</sub> group. In Table II the coordinates of the four oxygen nuclei of the phosphate group are given in the principal coordinate system, with the phosphorus nucleus as the origin. These coordinates were calculated from the X-ray coordinates by using the rotation matrix **R**<sup>(cp)</sup> (Figure 6). It is evident from Table II that only one of the two possible assignments of the chemical shielding tensor is in agreement with the symmetry of the PO<sub>4</sub> group.

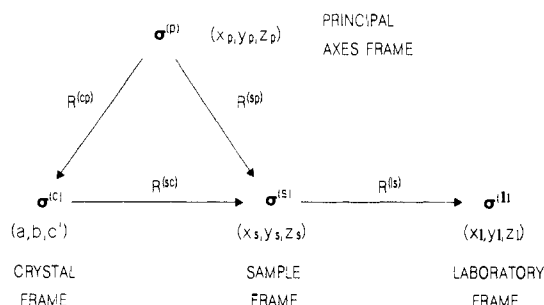


**Figure 6.** Summary of different coordinate systems (frames) used in this study. Also indicated are the rotation matrices transforming the <sup>31</sup>P chemical shielding tensor between different frames. The superscript of the rotation matrices indicates destination and origin of the transformation; e.g., **R**<sup>(cp)</sup> is the transformation matrix used to transform the <sup>31</sup>P chemical shielding tensor from the principal axes frame to the crystal frame.

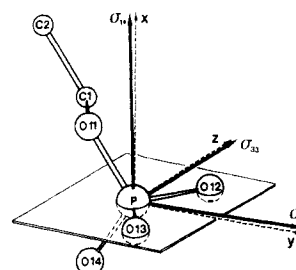


**Figure 7.** Orientation of the principal axes labeled σ<sub>11</sub>, σ<sub>22</sub>, and σ<sub>33</sub> (heavily printed) of the <sup>31</sup>P chemical shielding tensor in 1-hexadecyl-2-deoxyglycerophosphoric acid monohydrate (HPA2). Also included is a right-handed Cartesian coordinate system (x, y, z, dashed lines) which is directly related to the geometry of the PO<sub>4</sub> group. The y axis bisects the O12-P-O13 angle, x is perpendicular to the O12-P-O13 plane, and z completes the right-handed Cartesian coordinates.

**Table II.** Coordinates of the Relevant Nuclei in 1-Hexadecyl-2-deoxyglycerophosphoric Acid with Respect to the Principal Axes Frame of the Phosphorus Chemical Shielding Tensor Centered at the Phosphorus Nucleus<sup>a</sup>

| nucleus | coordinates, Å  |                 |                 |
|---------|-----------------|-----------------|-----------------|
|         | σ <sub>11</sub> | σ <sub>22</sub> | σ <sub>33</sub> |
| P1      | 0               | 0               | 0               |
| O11     | 1.16 (0.28)     | -1.02 (1.46)    | -0.09 (0.43)    |
| O12     | 0.12 (0.96)     | 0.79 (-0.66)    | 1.33 (1.03)     |
| O13     | -0.03 (-0.44)   | 0.80 (0.01)     | -1.26 (-1.42)   |
| O14     | -1.30 (1.33)    | -0.79 (-0.80)   | 0.09 (0.08)     |

<sup>a</sup> Values are given for the preferred and in parentheses for the rejected assignment of the two measured phosphorus chemical shielding tensors.

Similar arguments have been used to assign the chemical shielding tensors in phosphoethanolamine,<sup>5</sup> barium diethyl phosphate,<sup>2</sup> deoxycytidine 5'-monophosphate,<sup>10</sup> L-O-serine phosphate, and 3'-cytidine monophosphate.<sup>11</sup>

#### 4. Discussion

These measurements represent the first determination of the <sup>31</sup>P chemical shielding tensor in a phospholipid molecule. The orientation of the <sup>31</sup>P chemical shielding tensor of HPA2 with

(5) Kohler, S. J.; Klein, M. P. *Biochemistry* **1976**, *15*, 967-973.  
 (6) Mehring, M. *High Resolution NMR Spectroscopy in Solids*; Springer: Berlin, 1976.  
 (7) Veeman, W. S. *Prog. NMR Spectrosc.* **1984**, *16*, 193-235.  
 (8) Kohler, S. J.; Ellett, J. D.; Klein, M. P. *J. Chem. Phys.* **1976**, *64*, 4451-4458.  
 (9) Van Calsteren, M.-R.; Birnbaum, G. I.; Smith, I. C. P. *J. Chem. Phys.* **1987**, *86*, 5405-5410.  
 (10) Tutunjian, P.; Tropp, J.; Waugh, J. *J. Am. Chem. Soc.* **1983**, *105*, 4848-4849.  
 (11) Kohler, S. J.; Klein, M. P. *J. Am. Chem. Soc.* **1977**, *99*, 8290-8293.  
 (12) The original monoclinic coordinates (a, b, c) (β = 100.48°) are converted to Cartesian coordinates (a, b, c).

**Table III.** Principal Values  $\sigma_{ii}$  (ppm) Relative to the External Reference of 85%  $\text{H}_3\text{PO}_4$  of the  $^{31}\text{P}$  Chemical Shielding Tensor Determined in Single Crystals or Crystal Powder of Monoclinic HPA2<sup>a</sup>

| compd                                 | origin         | $\sigma_{11}$   | $\sigma_{22}$  | $\sigma_{33}$  | $1/3\sum_i\sigma_{ii}$ |
|---------------------------------------|----------------|-----------------|----------------|----------------|------------------------|
| HPA2                                  |                |                 |                |                |                        |
| molecule A                            | single crystal | $-52.1 \pm 0.7$ | $-2.0 \pm 0.7$ | $57.6 \pm 0.7$ | 1.16                   |
| molecule B                            | single crystal | $-54.0 \pm 0.7$ | $-2.2 \pm 0.7$ | $58.5 \pm 0.6$ | 0.77                   |
| molecules A and B                     | crystal powder | -54.4           | -0.4           | 54.6           | -0.07                  |
| phosphoethanolamine <sup>b</sup>      | single crystal | -67             | -13            | 69             | -3.7                   |
| barium diethyl phosphate <sup>c</sup> | single crystal | -75.9           | -17.5          | 109.8          | 5.5                    |

<sup>a</sup> For comparison the principal values  $\sigma_{ii}$  of phosphoethanolamine and barium diethyl phosphate are included. <sup>b</sup> From ref 5. <sup>c</sup> From ref 2.

respect to the phosphate group is depicted in Figure 7. The rotation matrix, with the nine direction cosines, relating the principal axis frame of this tensor to the crystal frame ( $a$ ,  $b$ ,  $c$ '), cf. Figure 6), is given in Table I.

As seen in Figure 7 the principal axes are clearly related to the P-O bonds. To emphasize this correlation a Cartesian coordinate system,  $xyz$  (dashed lines), is included in Figure 7. These coordinates were chosen so that  $y$  bisects the O13-P-O12 angle,  $x$  is perpendicular to the O13-P-O12 plane, and  $z$  lies in the O13-P-O12 plane and is orthogonal to  $x$  and  $y$ . The principal axes of the  $^{31}\text{P}$  chemical shielding tensor of HPA2 coincide within the accuracy of the measurement ( $1-2^\circ$ ) with the  $xyz$  frame (Figure 7). Furthermore, the direction of the least shielded tensor component  $\sigma_{11}$  is parallel to the O14-O11 vector, and that of the most shielded tensor component  $\sigma_{33}$  is parallel to the O13-O12 vector. The precise orientation of  $\sigma_{22}$  with respect to the plane O13-P-O12 (see square in Figure 7) becomes clear considering the following angles:  $\sigma_{22}$ -P-O12 =  $59.0^\circ$ ,  $\sigma_{22}$ -P-O13 =  $58.0^\circ$ ,  $\sigma_{22}$ -P-O11 =  $125.9^\circ$ ,  $\sigma_{22}$ -P-O14 =  $125.9^\circ$ ; accordingly  $\sigma_{22}$  dissects both the angles O13-P-O12 and O11-P-O14 almost precisely and lies about  $2^\circ$  above the square plane (O13-P-O12) shown in Figure 7.

The least shielded component is in the O14-P-O11 plane containing the P-O11 ester bond with single-bond character. The uncertainty in the determination of the P-O bond length by X-ray diffraction is  $\pm 0.06 \text{ \AA}$ .<sup>4</sup> Unfortunately, this accuracy does not allow the unambiguous assignment of the remaining oxygens. However, inspection of the P-O distances of both the monoclinic and triclinic crystal forms of HPA shows that on the average the P-O13 and P-O12 distances are shorter than the other two P-O distances. This would give rise to a higher electron density in the O13-P-O12 plane, in which the most shielded tensor components  $\sigma_{33}$  and  $\sigma_{22}$  are located.

The orientation of the  $^{31}\text{P}$  chemical shielding tensor of HPA2 is in good agreement with that of deoxycytidine 5'-monophosphate,<sup>10</sup> L-O-serine phosphate, 3'-cytidine monophosphate,<sup>11</sup> and phosphoethanolamine.<sup>5</sup> These compounds are all phosphomonoesters like HPA. The single-crystal structures of the above compounds do allow the unambiguous assignment of the P-O bonds. For instance, in the crystal structure of phosphoethanolamine, two P-O bonds, the P-O5 bond (O5, ester oxygen) and the P-O4 bond (O4, protonated), to use the original notation (cf. ref 5), are longer, having single-bond character, while the other two bonds, P-O2 and P-O3, are shorter, having partial double-bond character. From this the electron density around the P nucleus is expected to be concentrated in the O2-P-O3 plane, leaving the P nucleus relatively deshielded in the perpendicular O5-P-O4 plane. Consistent with the P-O bond character and the electron density distribution,  $\sigma_{22}$  and  $\sigma_{33}$  were found to be in the plane containing the two short P-O bonds. The least shielded component  $\sigma_{11}$  is almost precisely in the perpendicular O5-P-O4 plane, with single-bond character (cf. ref 5). The same consideration holds for the orientation of the  $^{31}\text{P}$  chemical shielding tensor

in deoxycytidine 5'-monophosphate,<sup>10</sup> L-O-serine phosphate, and 3'-cytidine monophosphate.<sup>11</sup>

In comparison, the principal axes of the  $^{31}\text{P}$  chemical shielding tensor for the phosphodiester barium diethyl phosphate deviate from the three reference axes  $x$ ,  $y$ , and  $z$ , with  $\sigma_{11}$  being  $7^\circ$  from the  $x$  axis,  $\sigma_{22}$   $13^\circ$  from the  $y$  axis, and  $\sigma_{33}$   $9^\circ$  from the  $z$  axis.<sup>2,3</sup> The corresponding deviations for HPA2 are, as mentioned above, about  $2^\circ$ .

The values of the tensor components of the three  $^{31}\text{P}$  chemical shielding tensor of HPA2, phosphoethanolamine, and barium diethyl phosphate discussed here are summarized in Table III. As is clear from this table and as shown in Figure 5, the two edges of the HPA2 powder spectrum are symmetrically arranged about the  $\text{H}_3\text{PO}_4$  reference, with the  $\sigma_{22}$  component almost coincident with the  $\text{H}_3\text{PO}_4$  reference. In the monoester phosphoethanolamine, the two extreme tensor components,  $\sigma_{11}$  and  $\sigma_{33}$ , are also symmetrically arranged about the  $\text{H}_3\text{PO}_4$  reference; however, the width of the phosphoethanolamine powder spectrum, expressed as  $|\sigma_{11} - \sigma_{33}|$ , is about 25 ppm larger than the width of the HPA2 spectrum. In contrast, the  $^{31}\text{P}$  powder spectrum of barium diethyl phosphate is asymmetrically arranged about the  $\text{H}_3\text{PO}_4$  reference; furthermore its width is about 50 and 75 ppm larger than that of phosphoethanolamine and HPA2, respectively (Table III). The principal values of the barium diethyl phosphate tensor are within 5% consistent with those derived from  $^{31}\text{P}$  powder spectra of diacylphosphatidylcholines, phosphatidylethanolamines, and phosphatidylserines.

It appears that the chemical shielding tensors determined for HPA2 and for barium diethyl phosphate are at present the best for phosphomono- and -diesters, respectively. However, their limitations should be borne in mind when employed in conformational studies of the phospholipid head group. Further work toward the determination of the  $^{31}\text{P}$  chemical shielding tensor in diacyl phospholipids is currently in progress.

**Acknowledgment.** This research has been supported by the Hoffmann-La Roche Stiftung and partly by the Swiss National Science Foundation (Grant No 3.223-0.85). We are indebted to Dr. U. Haerberlen of the Max-Planck-Institute in Heidelberg and Dr. R. G. Griffin of the Massachusetts Institute of Technology in Cambridge for valuable discussions. The goniometer probe assembly was built by Mr. Joseph Eisenegger and Mr. Thomas Schneider.

**Note Added in Proof:** Most recently, the  $^{31}\text{P}$  chemical shielding tensor of (2-aminoethyl)phosphonic acid was determined by van Calsteren et al.<sup>9</sup> The orientation of this tensor is qualitatively similar to that of the mono- and diesters of phosphoric acid. There is, however, a reduction in the magnitude of the principal components  $\sigma_{11}$  and  $\sigma_{33}$ . This has been attributed to a decrease in the overall electron density due to the replacement of a P-O bond by a P-C bond.

**Registry No.** HPA, 87746-71-2.